J. Phys. B: At. Mol. Opt. Phys. 26 (1993) 2191–2200. Printed in the UK

Electron-collision-induced dipole transitions in Na Rydberg atoms: 30s–30p and 30s–29p absolute cross sections

R G Rolfes†, L G Gray, O P Makarov and K B MacAdam

Department of Physics and Astronomy, University of Kentucky, Lexington, KY 40506-0055, USA

Received 6 November 1992, in final form 14 April 1993

Abstract. An experimental study of the depopulation of Na 30s Rydberg atoms under electron bombardment has been carried out. Electron energies E ranged from 105 to 660 eV corresponding to collision velocities 80 to 200 times the mean orbital speed of the excited 30s electron. The collision-induced final states were identified by means of selective field ionization (SFI). 30p, 29p, and a small trace of 28p were clearly observed in the adiabatic SFI distributions. Collision-induced diabatic SFI signals were absent, in contrast with a previous study that used slow ionic projectiles. 30s–30p and 30s–29p absolute cross sections were obtained from measurements of the collisional depopulation of the 30s state and measurements of the electron-beam current-density profiles. The cross sections ranged from 0.33 to 1.69×10^{-10} cm^2. The results agreed with calculations based on the dipole approximation with first-order perturbation theory and the Born approximation. Cross sections were also measured in external electric fields up to 15.75 V cm^{-1} for the higher collision energies (422 to 660 eV), but unlike the previous study no field dependence of cross sections or final-state distributions was apparent.

1. Introduction

Experiments on collisions between highly excited Rydberg atoms and charged particles have significance in the study of both astrophysical and laboratory plasmas. State-changing collision cross sections can be used to test the physical assumptions in plasma models. Recent work on collisions of Rydberg atoms with singly charged positive ions has concentrated on collision energies in the velocity matching region (Rolfes *et al* 1988, 1992, McAdam *et al* 1981, 1985, 1987). This is a difficult region for theory where few approximations can be made.

Few experiments on state-changing collisions at high reduced velocities $\bar{v} = v_{\text{projectile}}/v_{\text{Bohr}}$ have been undertaken. ($v_{\text{Bohr}} = n^{*-1}$ au is the Bohr orbital velocity of the Rydberg state with effective quantum number $n^* = n - \delta_l$. n is the principal quantum number, and δ_l is the quantum defect for states of orbital angular momentum l.) Foltz *et al* (1981) measured cross sections for the depopulation of sodium nd states ($n = 36$ to 50) by collisions with 25 eV electrons. Their results provided lower bounds to the total cross sections since they could not completely resolve their initial and final states by selective field ionization (SFI). Schiavone *et al* (1977, 1979) reported absolute cross sections for l-change between fast (30 to 300 eV) electrons and rare-gas Rydberg atoms. They detected high-l Rydberg states after collisions between electrons and ground state atoms. They assumed that the high l values resulted from l-change collisions occurring in the electron beam after

† Permanent address: Division of Science and Mathematics, Transylvania University, Lexington, KY 40508, USA.

0953-4075/93/142191+10$07.50

an initial direct excitation. Delpech *et al* (1977) and Devos *et al* (1979) have investigated n-changing collisions in helium by electron impact. They measured rate coefficients for induced transitions among Rydberg levels $n = 8$ to 17 in a helium afterglow.

Although most theoretical work at high collision velocities has concentrated on n change in hydrogen, Percival and Richards (1977) have given cross section formulae for nl to $n'l'$ transitions applicable for any atom. Their method uses the dipole approximation and first order perturbation theory and also uses the sudden approximation to account for the influence of other nearby 'resonant' states. Their C-region formulae are expected to be valid for electron collision energies greater than one Rydberg ($R = 13.6$ eV). Shevelko *et al* (1976) have used the Born approximation to develop a simple formula for nl to nl' cross sections. Herrick (1978) has used the high-energy impact-parameter formulation of Pengelly and Seaton (1964) to calculate nl to nl' cross sections for electron collisions with helium atoms. Beigman and Syrkin (1986) have obtained an approximation formula for l change cross sections applicable to Na Rydberg states that matches the Born approximation in the high-velocity limit and a normalized Born approximation near the cross section maximum.

In this paper we present experimental absolute cross sections for 30s–30p and 30s–29p transitions under high-velocity electron impact in the process

$$e^- + Na(30s) \rightarrow e^- + Na(n'l'). \tag{1}$$

The results are compared to calculations from the theories cited above and to the plane-wave Born approximation. Measurements are also reported for collisions in weak electric fields up to 15.75 V cm^{-1} at the higher collision velocities. The latter measurements were undertaken because a recent study (Rolfes *et al* 1992) of Na^+ collisions with Na 36s and 30p Rydberg atoms at velocities near the electronic orbital velocity had revealed strong dependences of the final-state distribution on electric fields that were even weaker than these.

The apparatus and experimental method are described in section 2. In section 3 the absolute cross section measurements are presented along with a discussion of statistical and systematic errors. Section 4 contains comparison with theory along with discussion and conclusions.

2. Experimental method

The apparatus shown schematically in figure 1 has been described in detail in previous papers (MacAdam *et al* 1981, Rolfes *et al* 1988, 1992). Two pulsed dye lasers were used for stepwise excitation of Na atoms in an atomic beam to the 30s state. The excited atoms occupied a volume of a few mm^3 midway between horizontal condenser plates separated by 1.27 cm. The atoms drifted with thermal velocities perpendicular to an electron beam that was produced by a gun taken from a type 3RP1 cathode ray tube. The total beam current was monitored by a deep Faraday cup FC1 positioned behind the collision region. In separate measurements a miniature movable shielded Faraday cup FC2 with aperture 2.207 mm^2 was inserted between the condenser plates. The midplane electron beam current density j was scanned at each kinetic energy and for each total FC1 current and interaction-region electric field used in the collision experiments and found to be uniform over the entire region of the collisions.

The 30s state was photoexcited in nominally zero electric field from the $3^2P_{3/2}$ intermediate state. At 0.16 μs after excitation a negative rectangular voltage pulse

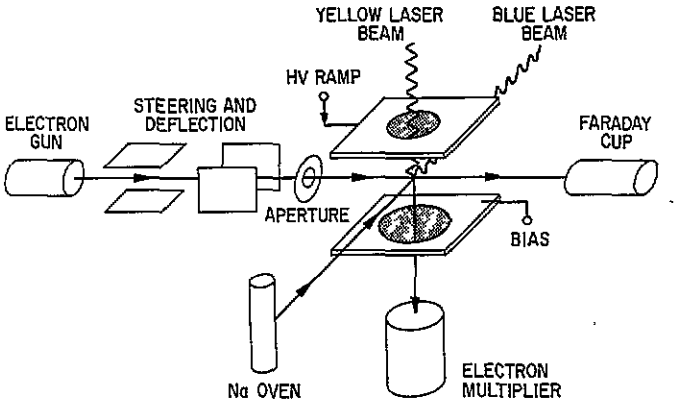

Figure 1. Apparatus (schematic).

(1000 V μs^{-1} slew rate) was applied to the bottom condenser plate to establish a steady field, except in the zero-field measurements, throughout the collision exposure time. Following termination of the electron beam by deflection, no later than 5.5 μs after the laser flash, a positive linear high-voltage ramp (Fuqua and MacAdam 1985) was applied to the upper plate for selective field ionization of the Rydberg atoms (Jeys *et al* 1980, Kleppner *et al* 1983). Ions were swept downward through a fine mesh into a discrete-dynode electron multiplier operated in current mode. Signals from the multiplier were recorded by an 8-bit 50 megasample-per-second transient digitizer.

The slew rate of the linear ramp was 107 V cm^{-1} μs^{-1}. This allowed complete time separation of the adiabatic field ionization (ASFI) profiles corresponding to the 30s and 30p states (see figure 2). The 30s and 29p ASFI profiles could not be completely resolved at any slew rate. (It can be seen in figure 2 that the second peak of the 30s signal is aligned with the largest peak of 29p.)

Figure 3 presents typical ASFI signals from the 30s parent state with the electron beam gated off and on. The third trace in the figure shows the difference of these two. It can be seen that the depopulation of 30s was accompanied by an increase in both the 30p and 29p populations, with the increase in the 29p partially masked because of the overlap of 30s and 29p ASFI signals. Note that some 30p and 29p population was present with electrons gated off due to dipole transitions out of the 30s caused by black-body radiation. The increase in 30p and 29p accounted for approximately 98% of the 30s collisional depopulation (a very small increase to 28p can be seen in the bottom trace of figure 3). No diabatic field ionization signals (DSFI) were detected for any electron energy used. The shapes of ASFI signals did not change in any way that would indicate dipole-forbidden transitions.

Depopulation cross sections were determined from the fractional decrease in ASFI signal using two integration windows on the 30s profile. A 60 ns window (A) was centred on the largest 30s peak and extended roughly between its half-intensity points. Window A enclosed about 30% of the signal attributable to the 30s state. It also enclosed 10.4% of the signal due to the overlapping 29p state and 2.5% of the 30p signal. A 420 ns window (B) was also chosen to encompass nearly the entire ASFI distribution of both the 30s (70%) and 29p (69%) states and about 11% of the 30p and 31s states while excluding entirely all other s and p states. Roughly speaking the percentage decrease in window A allowed the determination of the combined inelastic cross section to all states (other than 30s), and the decrease in window B yielded the cross section to all states other than 29p (and 30s), i.e.

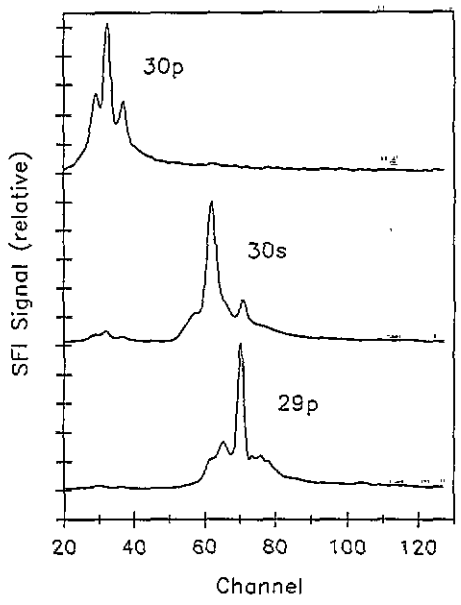

Figure 2. Experimental adiabatic SFI profiles for 30p, 30s and 29p (electron beam off) obtained by tuning the laser successively to each state.

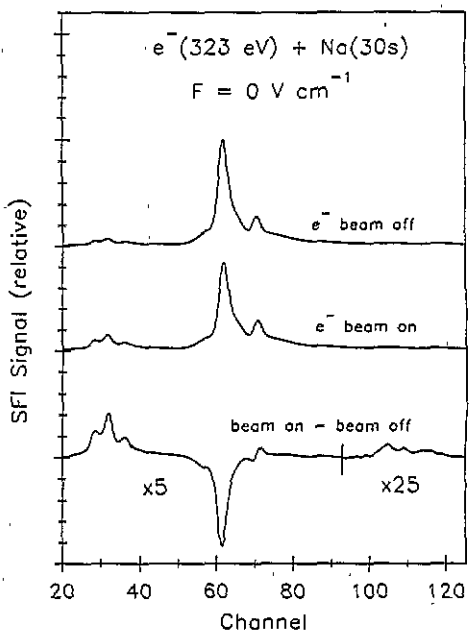

Figure 3. SFI profiles for 30s parent state with electron beam gated on and off. (The (beam on)–(beam off) trace shows that depopulation of 30s is primarily to 30p (near channel 90) and 29p (channels 25–35), with a small indication of transfer to 28p (channels 100–120). In the lower trace, the vertical scale has been expanded by factors 5 and 25 in the regions indicated as compared with the unexpanded scale of the other two traces. Channel spacing is 20 ns.

primarily to 30p. The 30s–29p cross section could be estimated by subtracting the decrease in B from that in A.

This may be made quantitative, allowing for the overlapping SFI signals, as follows. S_i^{nl} is the measured ASFI signal of state Na(nl) in channel i, normalized so that $\sum_i S_i^{nl} = 1$. N^{nl} is the number of Rydberg atoms in state nl at the time of detection by SFI, and (off) or (on) indicates the state of the projectile beam during the interval before detection. Then the measured signals are represented by

$$S_i(\text{on}) = \sum_{nl} N^{nl}(\text{on}) S_i^{nl} \tag{2a}$$

$$S_i(\text{off}) = N^{30s}(\text{off}) S_i^{30s}. \tag{2b}$$

We neglect the very small blackbody-excited population of non-30s states. The total integrated signals in A and B are therefore

$$I_A(x) = \sum_A S_i(x) \tag{3a}$$

$$I_B(x) = \sum_B S_i(x) \tag{3b}$$

where x = 'off' or 'on' and sums are carried out over channels i in windows A and B respectively. The conditions of window and SFI-profile overlap can be written

$$M_W^{nl} = \sum_W S_i^{nl} \tag{4}$$

for window W (A or B) and channels i contained in W. We have determined these overlap factors from the present data (figure 2) as

$$M_A^{30s} = 0.296 \qquad M_B^{30s} = 0.704 \tag{5a}$$

$$M_A^{30p} = 0.025 \qquad M_B^{30p} = 0.111 \tag{5b}$$

$$M_A^{29p} = 0.104 \qquad M_B^{29p} = 0.689. \tag{5c}$$

The fractional depopulation in W is

$$R_W = [I_W(\text{off}) - I_W(\text{on})]I_W(\text{off})^{-1}. \tag{6}$$

In the following, a primed summation over nl denotes a sum over all states except the initial 30s state. If we assume that

$$N^{30s}(\text{on}) + \sum_{nl}{}' N^{nl}(\text{on}) = N^{30s}(\text{off}) \tag{7}$$

which is experimentally confirmed within 2% over the complete measurement window, then from (2)–(7) we have

$$R_W = \sum_{nl}{}' k_{nl}\gamma_W^{nl} \tag{8}$$

where

$$k_{nl}\frac{N^{nl}(\text{on})}{N^{30s}(\text{off})} = \sigma(30s - nl)(j/e)\Delta t \tag{9}$$

and

$$\gamma_W^{nl} = 1 - M_W^{nl}/M_W^{30s}. \tag{10}$$

Δt is the exposure time of the Rydberg-atom target to the electron beam, and $-e$ is the electron charge. If all states other than the explicitly observed 30s, 30p and 29p are neglected (three-state model) cross sections σ(30s–30p) and σ(30s–29p) can thus be obtained from the measured depopulations by solving two equations of the form (8) for the two unknown cross sections. In view of the values of overlap factors (5), R_B measures (primarily) 30s–30p events and $R_A - R_B$ measures 30s–29p events. In writing (9) we have taken a small-signal approximation and have neglected multiple collisions, i.e. reverse transitions back into 30s or multi-step transitions among the considered levels. A slope method (Rolfes *et al* 1988) was used to determine the rate of decrease of population per unit exposure time of the target atoms to the electron beam, $R_W/\Delta t$, and thus to determine the overlap-weighted cross sections for each window. By this procedure, and by using Δt up to 5.5 μs, the inferred cross section was made independent of any constant unknown offset in the beginning or ending of the exposure interval.

3. Experimental results

Measured cross sections for the 30s–30p and 30s–29p transitions are presented in table 1. Seven kinetic energies from 105 to 660 eV were chosen that correspond to equally spaced reduced velocities $\tilde{v} = 80$ to 200. For measurements in non-zero external electric field F, the nominal energies must be corrected downward by 0.635 eV per V cm^{-1} to allow for deceleration of the electron beam into the target region. The electron beam was noticeably deflected by this transverse field at energies below 422 eV, so only zero-field cross sections are given at lower energies. Above 15.75 V cm^{-1} (20 V across the plates) a strong signal from resonant Rydberg–Rydberg collisions (Safinya *et al* 1981, Gallagher *et al* 1982) obliterated the electron collision signals and prevented studies at higher fields. (The earlier work of Rolfes *et al* (1992) was not troubled by this effect because cross sections in that study were two orders of magnitude larger, and a less dense Na beam could be used. The Rydberg–Rydberg collision rate depends on the *square* of the beam density.)

Table 1. Measured absolute cross sections for 30s–30p and 30s–29p transitions. Figures shown in parentheses are one-standard-deviation statistical uncertainties in the final digit shown. Additional systematic error is expected to be less than 25%. Energies E for $F > 0$ must be corrected downward slightly from the values in column 1 as described in the text.

Electron energy E (eV)	Reduced velocity $\tilde{v}$	Electric field F (V cm^{-1})	σ(30s–30p) (10^{-10} cm^2)	σ(30s–29p) (10^{-10} cm^2)
105	79.6	0	1.69(31)	0.94(71)
165	99.8	0	0.95(17)	0.54(38)
237	119.6	0	0.81(17)	0.55(38)
323	139.6	0	0.67(17)	0.44(38)
422	159.6	0	0.66(17)	0.52(38)
		3.15	0.73(17)	0.46(38)
		6.30	0.53(17)	0.47(38)
		9.45	0.43(17)	0.42(38)
		12.60	0.39(17)	0.41(38)
		15.75	0.41(17)	0.42(38)
531	179.0	0	0.51(17)	0.62(38)
		3.15	0.33(17)	0.65(38)
		6.30	0.52(17)	0.58(38)
		9.45	0.46(17)	0.71(38)
		12.60	0.50(17)	0.55(38)
		15.75	0.33(17)	0.48(38)
660	199.6	0	0.57(17)	0.53(38)
		3.15	0.51(17)	0.60(38)
		6.30	0.52(17)	0.54(38)
		9.45	0.46(17)	0.51(38)
		12.60	0.51(17)	0.54(38)
		15.75	0.52(17)	0.57(38)

The measured depopulations were generally less than 10% for all beam exposure times. As a result, the statistical uncertainties due to random fluctuations in laser frequency and intensity and in electron-gun operating conditions were large. Statistical uncertainties given in the table are averaged values (except at $E = 105$ eV) over the fields and energies used. The uncertainties for 30s–29p cross sections are greater than for 30s–30p because the cross section depends on the difference of two larger signals. Systematic error due to uncertainty

in the overlap of the crossed atomic, laser and electron beams was estimated to be less than 25%. For integration times much shorter than the radiative lifetimes of the states registered in windows A and B, no correction for radiative decay is necessary at the present level of accuracy. The black-body-corrected radiative lifetimes (410 K) of 30s, 30p and 29p states may be estimated from the calculations of Theodosiou (1984) to be 18, 52 and 48 μs, respectively.

4. Discussion

The measured zero-field 30s–30p cross section is plotted against E/R (where $R = 13.6$ eV) in figure 4, along with calculations using the published theories of Percival and Richards (1977) (PR), Shevelko *et al* (1976) (SUV) and Herrick (1978). The radial matrix element calculations of Edmonds *et al* (1979) were used in conjunction with both the PR and SUV theories. Both of these theories gave essentially the same results and are represented by the same line in the figure. A straightforward plane-wave Born approximation (PWBA) (Mott and Massey 1965) using the Coulomb approximation (Bates and Damgaard 1949) for the calculation of radial integrals has been provided by Cavagnero (1993). The PWBA coincides with the PR and SUV curve in this energy range. The approximation formula of Beigman and Syrkin (1986) with appropriate allowance for the non-hydrogenic states (Syrkin 1993) also coincides here with PR.

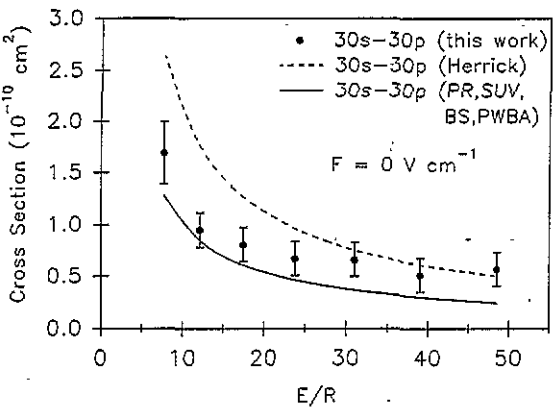

Figure 4. 30s–30p cross sections in zero field as a function of reduced collision energy E/R. Theoretical results from Herrick (1978) are shown. Results from Percival and Richards (1977) (PR), Shevelko *et al* (1976) (SUV), Beigman and Syrkin (1986) (BS) and the plane-wave Born approximation (Cavagnero 1993) are shown by a common curve.

The present measurements agree very well with the PR, SUV, PWBA and BS calculations. The results from Herrick are about a factor of two larger at all energies. The Herrick theory was developed to calculate nl–nl' cross sections for helium. When this theory was applied to sodium nd–nf transitions (Foltz *et al* 1982) it also agreed well with measurements and PR calculations. The lack of agreement in figure 4 could be due to this theory's use of hydrogenic radial wavefunctions. The quantum defects of sodium ns and np states (about 1.35 and 0.85, respectively) show that these states are distinctly non-hydrogenic.

Both the Herrick and SUV theories were constructed specifically for transitions without change of n, so the measured zero-field 30s–29p cross section is compared only to the PR, PWBA and BS calculations in figure 5. There is reasonable agreement between experiment and theory within the relatively large statistical uncertainty of the data.

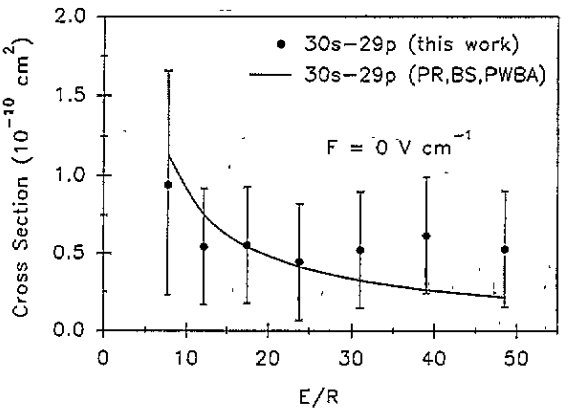

Figure 5. 30s–29p cross sections in zero field as a function of E/R. Notation as in figure 4.

As suggested by figure 3 and predicted by PWBA, the 30s–28p cross section is 50 to 60 times smaller than the 30s–30p and 30s–29p cross sections. However, the 30s–29d cross section predicted by PWBA is about 5% as large as those to 30p and 29p, and SFI signals for the 29d state would be lost under the much stronger 30s and 29p signals. In order to estimate the sensitivity of the present results to inelastic processes neglected in the three-state model, we have carried out a Born-corrected analysis of the data, using estimated overlap factors and PWBA cross sections (Cavagnero 1993) for seven other states whose SFI signals would appear in the measured range of channels and whose cross sections vary from about 1% to 5% of the two large cross sections reported here. This ten-state model includes: 29d, 30d, 31p, 28d, 28p, 31s and 29s, in order from largest to smallest cross section. The Born-corrected analysis yields a 30s–30p cross section about 9% smaller than the three-state analysis, and the 30s–29p cross section is unchanged within 1%. We take these as indications of the possible systematic error caused by the neglect of unmeasured states, and we note that the errors are smaller than the quoted statistical error bars.

The cross section ratio $\sigma_{30p}/\sigma_{29p}$ calculated from PR is independent of collision energy over the range considered and has the value 1.13. Our zero-field results also show this ratio to be energy independent within the statistical uncertainties with an average value 1.39 ± 0.33. A downward trend with increasing energy is visible but is not statistically significant.

The field dependence of the measurements is illustrated at 660 eV in figure 6. The ratio $\sigma_{30p}/\sigma_{29p}$ appears constant within the accuracy of the present work. Figure 7 shows that the energy separation between 30s and 30p increases slightly with increasing field, while that between 30s and 29p decreases, and this suggests that the cross section ratio may slightly decrease at higher fields. The figure also demonstrates that in the range $0 \leqslant F \leqslant 15.75$ V cm^{-1} very little p character is mixed into the adjacent n manifolds, and this may explain the absence of final-state signals other than the s and p states observed. Based

on the study of Na^++Na(36s) collisions near $\tilde{v} = 1$ (Rolfes *et al* 1992) a significant field dependence of the electron-impact cross sections might be found above $F = 60$ V cm^{-1}, unless the very rapid passage of the projectile causes a completely diabatic behaviour in the region of avoided crossings of the 30s state with the $n = 29$ manifold above 60 V cm^{-1} that is shown in figure 7.

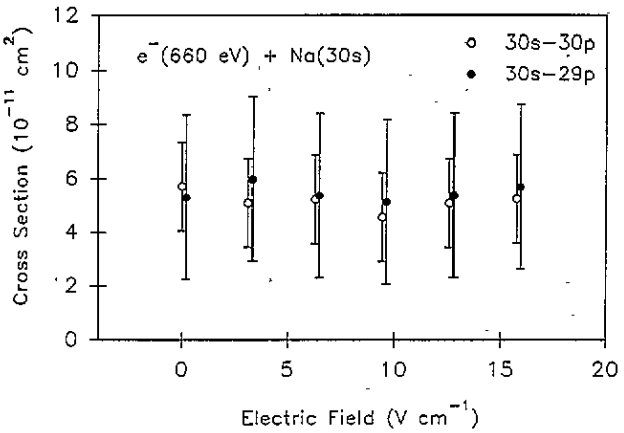

Figure 6. Measured 30s–30p and 30s–29p cross sections as a function of applied electric field strength for electron collision energy 660 eV.

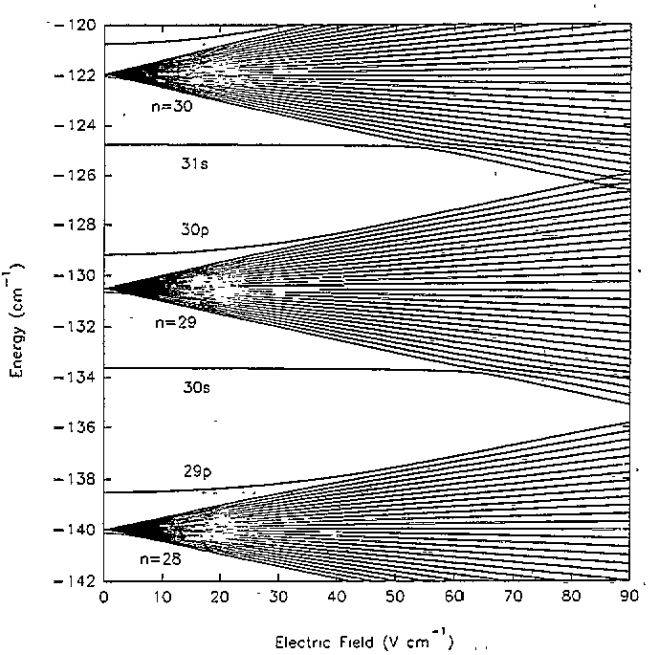

Figure 7. Na Stark energy levels ($m = 0$) in the vicinity of the 30s state.

In the work of Rolfes *et al* (1992), which encompassed a range of reduced velocities between 0.6 and 1.4, the collision-induced transitions from Na(36s) and Na(30p) states were distinctly dipole-forbidden. Both s and p states were driven into a range of sublevels mainly belonging to the energetically nearest manifold. The present work covered a reduced velocity range of 80 to 200, and transitions from 30s only to energetically nearby p levels were observed. The results provide the first experimental state-to-state cross sections for Rydberg atom transitions induced by fast electron impact and indicate that the plane-wave Born approximation and closely related models that include the significant quantum defects of non-hydrogenic states are reliable in this energy region. Future work will concentrate on finding the region of reduced velocities where the transition from dipole-forbidden to dipole-allowed behaviour occurs.

Acknowledgments

We are grateful for helpful discussions with M Syrkin and for PWBA calculations by Y Zheng and M Cavagnero. This work was supported in part by the National Science Foundation under Grant No PHY-9122377.

References

Bates D R and Damgaard A 1949 *Phil. Trans. R. Soc.* A **242** 101
Beigman I L and Syrkin M I 1986 *Lebedev Institute (Moscow) Physics Report* 7 pp 13–16 (Engl. transl. 1986 (New York: Allerton)
Cavagnero M G 1993 unpublished
Delpech J-F, Boulmer J and Devos F 1977 *Phys. Rev. Lett.* **39** 1400
Devos F, Boulmer J and Delpech J-F 1979 *J. Physique* **40** 215
Edmonds A R, Picart J, Tran Minh N and Pullen R 1979 *J. Phys. B: At. Mol. Phys.* **12** 2781
Foltz G W, Beiting E J, Jeys T H, Smith K A, Dunning F B and Stebbings R F 1982 *Phys. Rev.* A **25** 187
Fuqua W L III and MacAdam K B 1985 *Rev. Sci. Instrum.* **56** 385
Gallagher T F, Safinya K A, Gounand F, Delpech J F, Sandner W and Kachru R 1982 *Phys. Rev.* A **25** 1905
Herrick D R 1978 *Mol. Phys.* **35** 1211
Jeys T H, Foltz G W, Smith K A, Beiting E J, Kellert F G, Dunning F B and Stebbings R F 1980 *Phys. Rev. Lett.* **44** 390
Kleppner D, Littman M G and Zimmerman M L 1983 *Rydberg States of Atoms and Molecules* ed R F Stebbings and F B Dunning (New York: Cambridge University Press) p 73
MacAdam K B, Rolfes R G and Crosby D A 1981 *Phys. Rev.* A **24** 1286
MacAdam K B, Rolfes R G, Sun X, Singh J, Fuqua W L III and Smith D B 1987 *Phys. Rev.* A **36** 4254
MacAdam K B, Smith D B and Rolfes R G 1985 *J. Phys. B: At. Mol. Phys.* **18** 441
Mott N F and Massey H S W 1965 *Theory of Atomic Collisions* vol 2, 3rd edn (Oxford: Oxford University Press) pp 327–9
Pengelly R M and Seaton M J 1964 *Mon. Not. R. Astron. Soc.* **127** 165
Percival I C and Richards D 1977 *J. Phys. B: At. Mol. Phys.* **10** 1497
Rolfes R G, Gray L G and MacAdam K B 1992 *J. Phys. B: At. Mol. Opt. Phys.* **25** 2319
Rolfes R G, Smith D B and MacAdam K B 1988 *Phys. Rev.* A **37** 2378
Safinya K A, Delpech J F, Gounand F, Sandner W and Gallagher T F 1981 *Phys. Rev. Lett.* **47** 405
Schiavone J A, Donohue D E, Herrick D R and Freund R S 1977 *Phys. Rev.* A **16** 48
Schiavone J A, Tarr S M and Freund R S 1979 *Phys. Rev.* A **20** 71
Shevelko V P, Urnov A M and Vinogradov A V 1976 *J. Phys. B: At. Mol. Phys.* **9** 2859
Syrkin M I 1993 private communication
Theodosiou C E 1984 *Phys. Rev.* A **30** 2881